Table S1: Strains and plasmids used in this study

Strain or plasmid	Description	Source or Reference
E. coli		
DH10B	F$^-$ *mcrA* Δ(*mrr–hsdRMS–mcrBC*) ϕ80d*lacZ* ΔM15 Δ*lacX74 deoR recA1 ara*D139 Δ(*ara leu*)7697 *galU galK rpsL endA1 nupG*	Invitrogen
BL21 (DE3)	F$^-$ *ompT gal dcm lon hsdS$_B$*($r_B^- m_B^-$) λ(DE3 [*lacI lacUV5-T7p07 ind1 sam7 nin5*]) [*malB*$^+$]$_{K-12}$(λ^S)	Invitrogen
M. smegmatis		
mc^{2}155	*ept-1*, efficient plasmid transformation mutant of mc^2 6	(1)
Δ*fsq*	mc^2 155 Δ*fsq*	This study
Δ*6368*	mc^2 155 Δ*MSMEG_6368*	This study
Δ*dosR*	mc^{2}155 with marked deletion of *MSMEG_3944*, Hyg^R	(2)
Plasmids		
pX33	pPR23 carrying a constitutive *xylE* marker; Gm^{r+}	(3)
pMind	Tetracycline inducible vector	(4)
pJEM*hyd3-lacZ*	pJEM15 fused to promoter region of the Hyd3 operon	(5)
pETMCSIII	T7 inducible vector	(6)
pETMCSIII-5243	T7 inducible vector for Fsq expression His-tagged	(7)
pLH1	pX33 containing flanking regions of *fsq* for deletion	This study
pLH2	pMind containing *fsq* gene with an artificial RBS	This study
pLH3	pX33 containing flanking regions of *MSMEG_6368* for deletion	This study

Table S2: Primers used in this study. Underlined text represents restriction enzyme recognition site used.

Primer Name	Sequence 5' – 3'
LH1	TTTTACTAGTAAGGTCGCCGAGGAGCGCAA
LH2	CGTCGGCGGTGGTGATCTGATCGCTCATGGAT
LH3	TCAGATCACCACCGCCGACGCCTCATGACC
LH4	AATTACTAGTGGCAGGTTCGGCAGCATCAC
LH5	AATTGGATCCGGAGGAATAATGAGCGATCAGATCACCACG
LH6	TTTTACTAGTGTCGAGCACGGAGAGCTGTT
LH7	CGTAGGGGGGATCCACTAGTCCCGGCATCAGGTTGTGCTT
LH8	GTGAAGAACCGCCCCGAGATCTCGTTCTCGCTGAGCACTG
LH9	CAGTGCTCAGCGAGAACGAGATCTCGGGGCGGTTCTTCAC
LH10	GCGGCCGCTCTAGAACTAGTCGGCTGGTACTTTCTGGTGT
LH11	TGTCAGTGCTCAGCGAGAAC
LH12	AACAGCACGCGATCACTCAT
LH13	GTCGCACATCTTCCCGATCA
LH14	ATGACGCTCCACCCCTGTTC
sigA fw	GACTCTTCCTCGTCCCACAC
sigA rev	GAAGACACCGACCTGGAACT
tgsfw	GATGCTGGCCACCAATGT
tgsrev	GCGTCGTAGTCGGAGATGAT
fsqCfw	ACCGCGCTGATGTCCAAACT
fsqCrv	GACGCAGTGGTGGATCTTGA

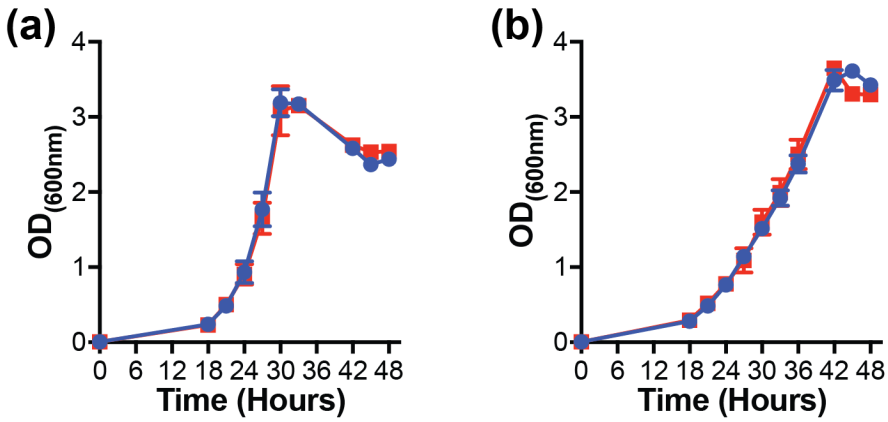

Fig. S1. Growth of *M. smegmatis* wild type (WT) compared to Δ*fsq* mutant under aerobic conditions. (a) Growth on HdB with 22 mM glycerol as the sole carbon and energy source. Average optical density of three biological replicates shown with standard deviation. (b) Growth on HdB with 30 mM succinate as the sole carbon and energy source. Average optical density of three biological replicates shown with error bars representing standard deviation.

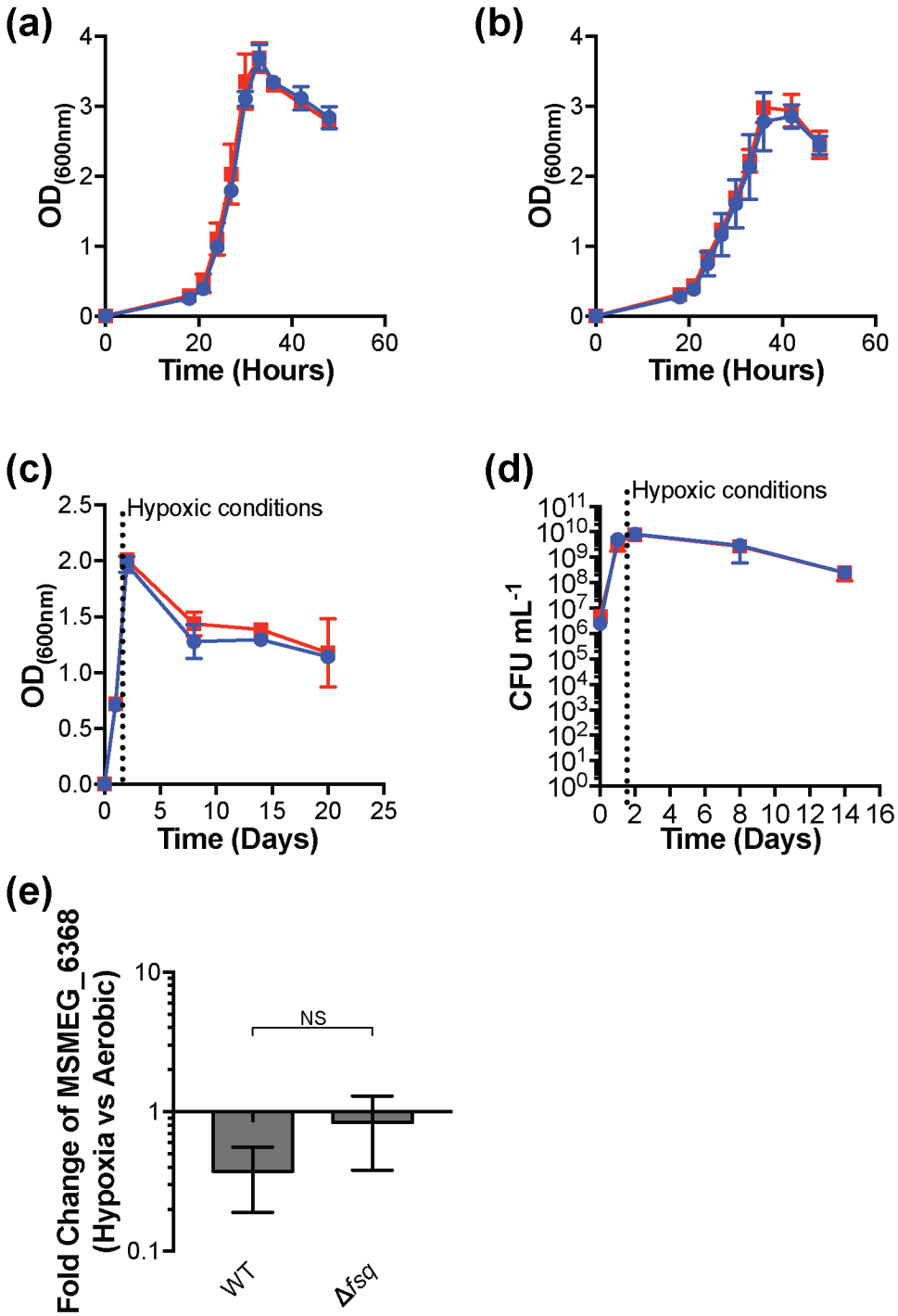

Fig. S2. MSMEG_6368 does not affect growth of *M. smegmatis*. Wild type (WT) blue circles, Δ6368 mutant red squares (a) Growth on HdB aerobically with 22 mM glycerol as the sole carbon and energy source. Average optical density of three biological replicates with error bars representing standard deviation. (b) Growth on HdB aerobically with 30 mM succinate as the sole carbon and energy source. Average of three biological replicates with error bars representing standard deviation. (c) Growth following entry into hypoxia measured by optical density. Average of three biological replicates with error bars representing standard deviation. (d) Survival following entry into hypoxia measured by colony forming units on agar plates. Average of three biological replicates with error bars representing standard deviation. (e) Comparison of expression ratio of *MSMEG_6368* in wild-type and Δ*fsq* mutant genetic backgrounds from cells harvested at 6 days growth in aerobic and hypoxic conditions. *SigA* was used as the reference gene. Error bars represent standard deviation of biological triplicate. Unpaired students t test. NS=$p<0.05$.

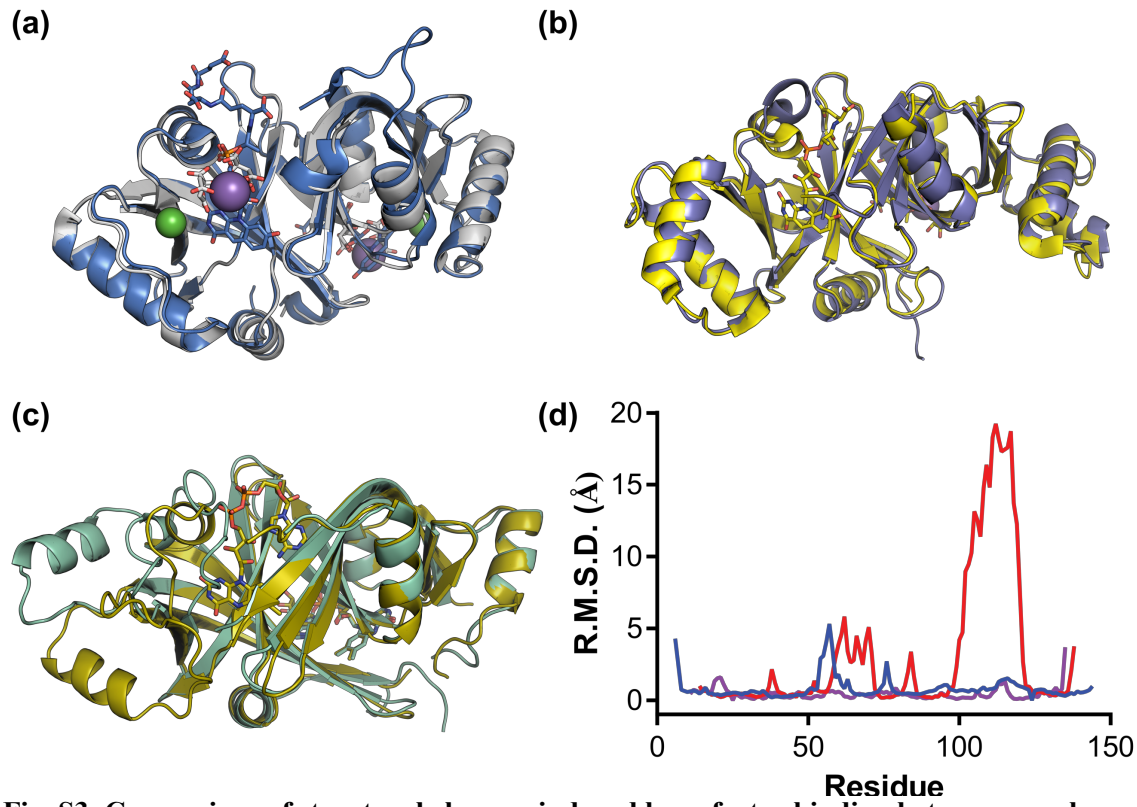

Fig. S3. Comparison of structural changes induced by cofactor binding between members of the FDOR superfamily (a) Overlay of rv2074 complexed with citrate (2ASF, white) and complexed with F_{420} (5JAB, blue). (b) Overlay of rv1155 apo structure (1W9A, purple) and complexed with F_{420} (4QVB, yellow). (c) Overlay of MSMEG_5243 partially complexed with FAD (OP dimer, light green) and fully complexed with FAD (AB dimer, gold). (d) R.M.S.D. of backbone residues between apo and holo complexes of rv2074 (purple), rv1155 (blue) and MSMEG_5243 (red).

Supplementary references

1. Snapper SB, Melton RE, Mustafa S, Kieser T, Jacobs WR, Jr. 1990. Isolation and characterization of efficient plasmid transformation mutants of Mycobacterium smegmatis. Mol Microbiol 4:1911-9.
2. O'Toole R, Smeulders MJ, Blokpoel MC, Kay EJ, Lougheed K, Williams HD. 2003. A two-component regulator of universal stress protein expression and adaptation to oxygen starvation in Mycobacterium smegmatis. J Bacteriol 185:1543-54.
3. Gebhard S, Tran SL, Cook GM. 2006. The Phn system of Mycobacterium smegmatis: a second high-affinity ABC-transporter for phosphate. Microbiology 152:3453-65.
4. Blokpoel MC, Murphy HN, O'Toole R, Wiles S, Runn ES, Stewart GR, Young DB, Robertson BD. 2005. Tetracycline-inducible gene regulation in mycobacteria. Nucleic Acids Res 33:e22.
5. Berney M, Greening C, Hards K, Collins D, Cook GM. 2014. Three different [NiFe] hydrogenases confer metabolic flexibility in the obligate aerobe Mycobacterium smegmatis. Environ Microbiol 16:318-30.
6. Neylon C, Brown SE, Kralicek AV, Miles CS, Love CA, Dixon NE. 2000. Interaction of the Escherichia coli Replication Terminator Protein (Tus) with DNA: A Model Derived from DNA-Binding Studies of Mutant Proteins by Surface Plasmon Resonance†. Biochemistry 39:11989-11999.
7. Ahmed FH, Carr PD, Lee BM, Afriat-Jurnou L, Mohamed AE, Hong NS, Flanagan J, Taylor MC, Greening C, Jackson CJ. 2015. Sequence-Structure-Function Classification of a Catalytically Diverse Oxidoreductase Superfamily in Mycobacteria. J Mol Biol 427:3554-3571.